Organic Electronics 13 (2012) 129–135

Contents lists available at SciVerse ScienceDirect

Organic Electronics

journal homepage: www.elsevier.com/locate/orgel

Enhancing photovoltaic response of organic solar cells using a crystalline molecular template

Wei Zhao [1], John P. Mudrick, Ying Zheng, William T. Hammond [2], Yixing Yang, Jiangeng Xue *

Department of Materials Science and Engineering, University of Florida, Gainesville, FL 32611, USA

ARTICLE INFO

Article history:
Received 12 May 2011
Received in revised form 3 October 2011
Accepted 23 October 2011
Available online 7 November 2011

Keywords:
Organic photovoltaic cells
Small molecules
Organic solar cells
Molecular template
Crystal structure

ABSTRACT

We demonstrate that a crystalline pentacene molecular templating layer considerably changes the morphology of the subsequently deposited lead phthalocyanine (PbPc) layer, resulting in an improved crystallinity at the early stages of growth of the PbPc film and a higher content of the triclinic phase. For bilayer PbPc (20 nm)/C_{60} (40 nm) organic solar cells with or without the pentacene templating layer, the use of the pentacene templating layer leads to a 48% enhancement in the short-circuit current without noticeably affecting the solar cell open-circuit voltage or fill factor. A copper or zinc phthalocyanine molecular templating layer also leads to enhanced photovoltaic response from the PbPc/C_{60} cells, though less significant than the pentacene template. The improved device performance originates from stronger absorption by the triclinic PbPc phase in the near infrared and the enhanced internal quantum efficiency over the entire spectrum where PbPc absorbs.

1. Introduction

The efficiency of organic solar cells has steadily increased in the past few years [1,2]; however significant research is still needed to further advance their performance to meet the requirement for commercial application. Compared to the inorganic semiconductors used as light absorbers in solar cells, the organic semiconductors in general have a larger band gap and a lack of absorption in the near infrared (NIR) wavelength region of the solar spectrum. Most reported organic solar cells have spectral response up to a wavelength of 800 nm, meaning that more than 40% of the solar power is not utilized. In order to broaden the spectral coverage and increase the short-circuit current, low-gap (E_g < 1.6 eV) organic semiconductors are desired to absorb long wavelength photons.

Among the available organic materials, phthalocyanines, particularly the non-planar ones such as lead phthalocyanine (PbPc), are notable for their absorption in the near infrared [3–7]. PbPc has been known for crystallizing either in monoclinic or triclinic phases, which possess different optical and electronic properties [8–10]. It is suggested that the intermolecular interaction is stronger than it is in the monoclinic phase due to a closer packing of the molecules, as revealed by X-ray diffraction and confirmed by theoretical calculations [10,11]. The triclinic phase of PbPc offers substantial absorption in the near infrared up to 1000 nm [7,10], thus making it a very interesting candidate for solar cell application.

Both monoclinic and triclinic phase coexist in the as-grown film by vacuum thermal evaporation [7,10]. The peak absorption for the monoclinic phase PbPc occurs at a wavelength of λ = 740 nm, whereas that for the triclinic phase is significantly red-shifted to λ = 890 nm [7]. Controlled growth of the PbPc film is of great importance in order to optimize the device performance. The crystallinity of the film and the ratio between the two phases can be tuned by varying the deposition rate and substrate temperature [7,10]. It was also reported that a phase transition for titanyl phthalocyanine can be realized by annealing the film in a solvent environment [12]. Most recently, structural tem-

* Corresponding author.
E-mail address: jxue@mse.ufl.edu (J. Xue).
[1] Current address: Polyera Corp., Skokie, IL 60077, USA.
[2] Current address: Intel Corp., Chandler, AZ 85226, USA.

1566-1199/$ - see front matter © 2011 Elsevier B.V. All rights reserved.
doi:10.1016/j.orgel.2011.10.016

plating achieved via applying a crystalline interlayer has been demonstrated to change the orientation of the subsequently deposited molecules [13] or the ordering of the polycrystalline overlayer [6]. In the present work, we show that crystal structures of the vacuum-deposited PbPc layer can be varied by using a crystalline pentacene templating layer on the substrate, and further demonstrate that the corresponding PbPc/C_{60} organic solar cell performance can be significantly enhanced.

2. Experimental methods

Organic thin films were grown on glass substrates precoated with a layer of indium-tin-oxide (ITO, sheet resistance ~20 Ω/□) in a high vacuum chamber (base pressure ~1×10^{-7} Torr). Metal phthalocyanines (metal = lead, zinc, and copper) and fullerene C_{60} were all purified at least once by the vacuum gradient sublimation methods [14]. The schematic device structure and energy level diagram of PbPc/C_{60} solar cells are illustrated in Fig. 1(a) and (b), respectively. All of the organic layers, including the pentacene (Fig. 1(c)) templating layer, the PbPc (Fig. 1(d)) donor layer, the C_{60} acceptor layer, and the BCP exciton-blocking layer [15,16] were successively deposited on the substrate, followed by the Al cathode. The thicknesses of these layers were monitored using quartz crystal microbalances and typical deposition rates were 0.3–2 Å/s with the substrate maintained at room temperature. The active device area was 0.04 cm^2, defined by the cross-bar geometry between the patterned electrodes. The devices were then encapsulated with epoxy and a cover glass in the nitrogen filled glove box before being exposed to air for testing. The encapsulation is critical for the device performance since PbPc is sensitive to oxygen [17]. Each batch could produce 16 devices with identical structures.

The optical absorption of the films from 300 to 1100 nm was obtained by measuring the transmittance and reflectance of the PbPc films upon monochromatic light incidence. The intensities of the light beams were measured using calibrated silicon photodetectors. The morphology of the PbPc films grown on Si (100) substrates was characterized in air using a Nanoscope III atomic force microscope (AFM) operated in the tapping mode. Ultrathin PbPc films were deposited at a rate of 0.01–0.02 Å/s for precise control of the thickness to investigate the very early stages of film growth. An Agilent 4155 semiconductor parameter analyzer was used to measure the current–voltage characteristics of the organic solar cells in the dark and under simulated AM 1.5G solar illumination from an Oriel solar simulator equipped with a Xe-arc lamp. An *unfiltered*, crystalline Si reference cell was used to measure the intensity of the solar simulator, which was adjusted to 1 sun to account for the spectral mismatch factor [18] of the ITO/PbPc (20 nm)/C_{60} (40 nm) device. External quantum efficiency (EQE) measurement was also taken at the short-circuit condition with a monochromatic light from a halogen lamp chopped at 400 Hz using a mechanical chopper.

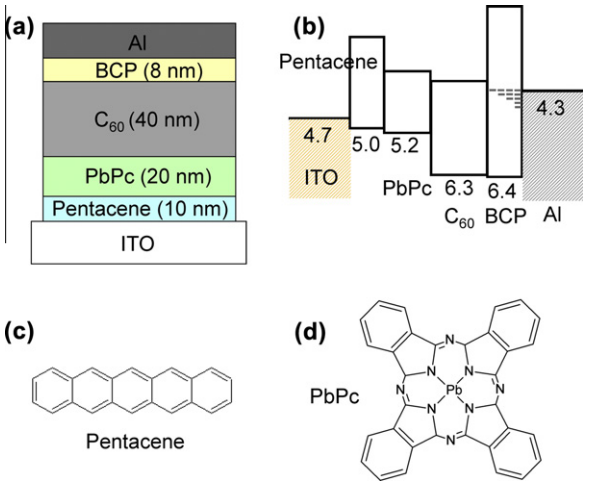

Fig. 1. Schematic device structure (a) and energy level diagram (b) of the PbPc/C_{60} organic solar cells. The molecular structures of pentacene and PbPc are shown in (c) and (d), respectively.

3. Results and discussion

3.1. Film absorbance

As mentioned above, the monoclinic and triclinic phases exhibit very different optical properties. A significant red-shift in the absorption occurs with the transition from the monoclinic to the triclinic phase upon thermal annealing of the film [10]. The phase information in turn is reflected in the optical absorption. The absorbance spectra of PbPc films deposited on ITO/glass substrate at various thicknesses, with or without a 10 nm thick pentacene templating layer are shown in Fig. 2. For the films on bare ITO (Fig. 2(a)), the spectrum of the 10 nm thick PbPc film is

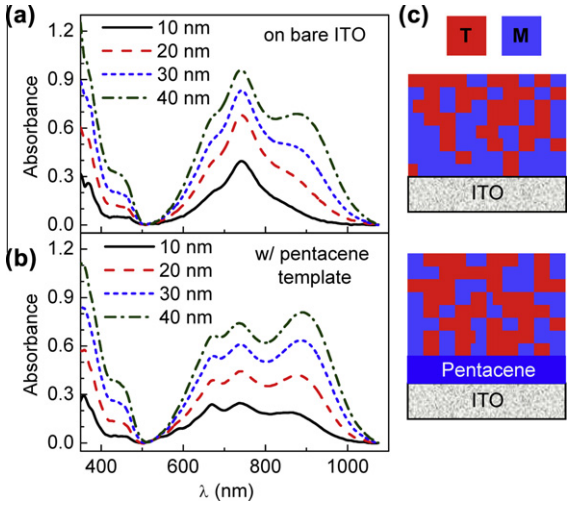

Fig. 2. Optical absorption spectra of PbPc films with thickness varying from 10 to 40 nm, deposited on the bare ITO surface (a) or on ITO substrates coated with a 10 nm thick pentacene molecular templating layer (b). The corresponding schematic phase maps are shown in (c) to illustrate difference in the distribution of the monoclinic (M) and triclinic (T) PbPc phases with or without the pentacene templating layer between ITO and PbPc. (For interpretation of the references to colour in this figure, the reader is referred to the web version of this article.)

composed of a prominent peak at around λ = 740 nm, corresponding to the absorption of the monoclinic phase, and a tail extending to above 900 nm [10]. As the thickness of the PbPc film increases, the peak corresponding to the absorption of the triclinic phase emerges at around λ = 890 nm, and its intensity increases at a faster rate than that of the monoclinic phase [10]. This suggests that the PbPc film directly grown on ITO is primarily composed of the monoclinic phase at the very beginning of film growth; however, the content of the triclinic phase increases with increasing film thickness. Our observation here is in excellent agreement with the X-ray diffraction measurements reported for the PbPc film deposited at slow rate and room temperature [7,10]. This phase distribution evolution is schematically illustrated in Fig. 2(c), which qualitatively describes the distribution of the two phases as the film thickness progresses.

When a 10 nm thick pentacene layer was deposited on ITO prior to the PbPc film deposition, the absorption spectra shown in Fig. 2(b) reveal that the triclinic phase coexists with the monoclinic phase at all PbPc film thicknesses. The intensity of both absorption peaks at λ = 740 and 890 nm increase simultaneously as the thickness of PbPc increases. Compared to the PbPc film deposited on the bare ITO substrate where the two phases have a gradient distribution in the film thickness direction, they are relatively homogenously distributed across the entire film as illustrated in Fig. 2(c).

3.2. Film morphology

According to the absorption measurement shown in Fig. 2, the most significant difference in the phase composition of PbPc films with or without the pentacene template occurs when the PbPc film is very thin. We thus look into the morphology of ultrathin PbPc films to assess the initial stages of film growth. Fig. 3(a) shows an AFM topographic image of 10 Å thick PbPc film on Si (100). The silicon surface was selected as the substrate instead of ITO due to its flatness so that even the sub-monolayer of PbPc can be easily assessed without interference of a rough surface. The film has a root mean square (RMS) roughness of 2.8 Å and shows incomplete coverage at this film thickness. Serpentine chains of domains with a typical size of 20 nm are uniformly distributed on the surface (also see the close-up in Fig. 3(b)). This suggests a high density and uniform nucleation of PbPc molecules on the bare Si substrate.

On the other hand, the PbPc film on the 50 Å thick pentacene templating layers shows remarkably different morphology. As shown in Fig. 4(a), pentacene molecules form the well-ordered dendrite crystalline multilayer structures on the silicon surface [19]. For the 2 Å thick sub-monolayer PbPc film (Fig. 4(b)), nearly all the PbPc molecules diffuse to the ledges of the pentacene terraces where they aggregate and form clusters. The surface coverage of PbPc on pentacene is significantly less than it is on the silicon. A close inspection of the line profile in Fig. 4(b) reveals that: (1) the height of a pentacene single layer is slightly less than 2 nm, in agreement with the length of the pentacene molecule and an upright standing configuration [19,20] which suggests that the crystal structure of the pentacene layers is not disturbed by the adsorption of PbPc; (2) the average footprint of a PbPc cluster is about 50 nm in diameter, significantly greater than that when PbPc was directly deposited on the silicon surface; (3) the height of these clusters varies from 5 to 10 nm even though the nominal film thickness is only 2 Å. As more PbPc was deposited (Fig. 4(c)–(e)), the size of each PbPc cluster does not increase appreciably. Instead, the density of PbPc clusters continues to increase at the ledges of the pentacene terraces until they are fully occupied, after which PbPc clusters develop from the ledges towards the center of the terraces.

Both the larger cluster size and a much higher RMS roughness (33 Å for the 10 Å film vs. 2.8 Å on the bare silicon) strongly suggest that the PbPc film on pentacene has better crystallinity than it has on the bare silicon substrate. The fact that the molecules migrate to the ledges of the pentacene terraces and then form large size clusters is very likely due to the weak interaction between the pentacene and PbPc molecules so that the adsorbed molecules are energetically mobile until they encounter the step edges where the interactions between the pentacene and PbPc molecules are sufficiently strong to immobilize them.

3.3. Device performance

Fig. 5(a) shows a comparison of the current density–voltage (J–V) characteristics under 1 sun (100 mW/cm^2) AM 1.5G illumination and the quantum efficiency spectra of PbPc (20 nm)/C_{60} (40 nm) devices without any template or with a 10 nm thick pentacene, CuPc, or ZnPc templating

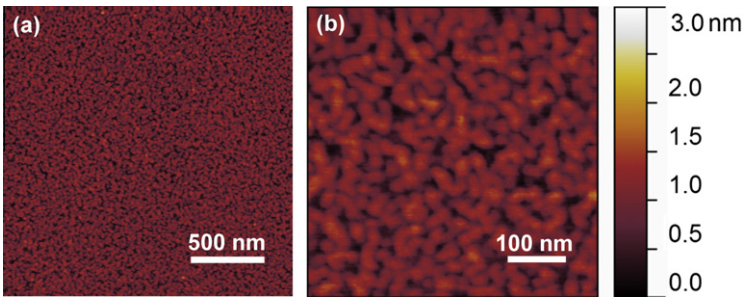

Fig. 3. AFM topographic images of 10 Å thick PbPc on Si (100) with a scan area of (a) 2 × 2 μm^2 and (b) 500 × 500 nm^2.

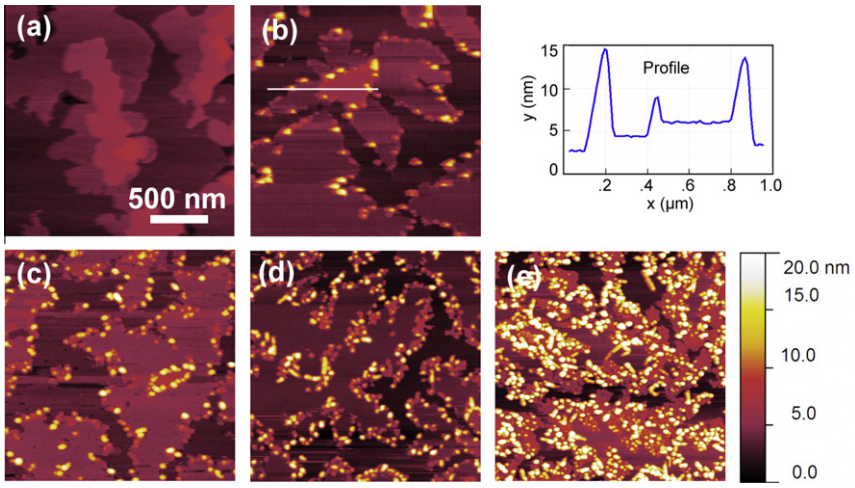

Fig. 4. AFM topographic images of PbPc films on a Si substrate coated with a 50 Å thick pentacene film. The nominal PbPc film thickness is (a) 0 Å, (b) 2 Å, (c) 5 Å, (d) 10 Å, and (e) 20 Å. The line profile in (b) shows the height of a single pentacene layer and the sizes of the PbPc clusters.

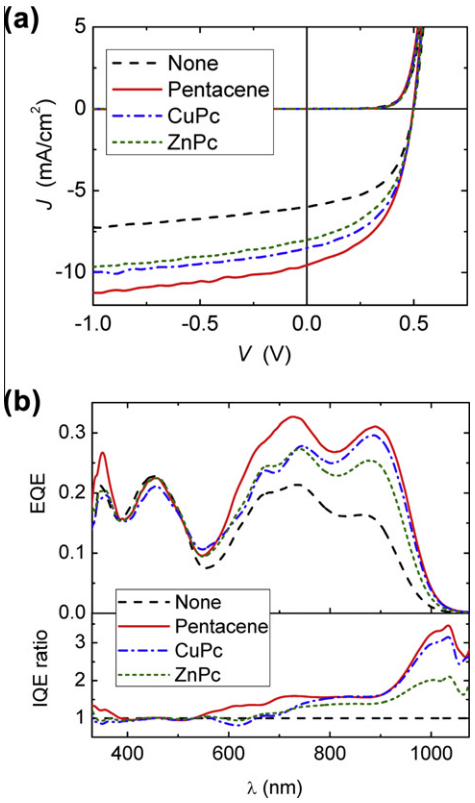

Fig. 5. (a) The current density–voltage (J–V) characteristics of a non-templated PbPc/C_{60} device and devices employing a pentacene, CuPc, or ZnPc templating layer, under 1 sun simulated AM 1.5G solar illumination. (b) The external quantum efficiency (EQE) spectra of the devices in (a) and the enhancement of the internal quantum efficiency (IQE) of the template devices over that for the non-templated device.

layer on the ITO substrate. Table 1 summarizes the photovoltaic performance parameters (short-circuit current density J_{SC}, open-circuit voltage V_{OC}, fill factor FF, and power conversion efficiency η_P) of these devices. The variation in device performance for more than 10 devices with the same structure from either the same batch or from different batches is typically no more than 5%. As shown in Table 1, the devices featuring a pentacene templating layer exhibit 48% higher J_{SC} than the devices without a template. With the same V_{OC} and a slightly decreased FF, the power conversion efficiency increases from $\eta_P = 1.57$–2.24% with the use of the pentacene template, equivalent to a net increase of 43%. Comparing the EQE spectra of these devices (shown in Fig. 5(b)), we see that the pentacene-templated device has a higher EQE than the non-templated device in the entire PbPc absorption region ($\lambda = 550$–1000 nm), which is more significant in the longer wavelength portion corresponding to the triclinic PbPc phase absorption. On the other hand, there is virtually no difference in the C_{60} absorption region ($\lambda = 400$–550 nm). From the J–V characteristics we also observe that the addition of the pentacene layer does not increase the series resistance of the device, which is attributed to the high hole mobility in pentacene and the close alignment of the highest occupied molecular orbital (HOMO) energies of pentacene and PbPc. It is also noted that the positive impact of a pentacene templating layer is present even with a 5 nm thick pentacene layer and a power conversion efficiency of $\eta_P = 2.00\%$ was obtained (compared to $\eta_P = 1.57\%$ for the device without the templating layer). With further increasing the pentacene templating layer thickness, the content of the triclinic PbPc phase increases leading to enhanced absorption in NIR; however, the absorption of pentacene also becomes more appreciable, which eventually deteriorates the solar cell performance. Ten nanometers was found to be the optimal thickness for the pentacene templating layer.

Note that we have adjusted the solar simulator intensity to account for the spectral mismatch factor [18] for the device without any template. By integrating the EQE spectrum of that device with the standard AM1.5G solar spectrum [21], we obtain a calculated J_{SC} in excellent agreement with the measured J_{SC} for that device (see Ta-

Table 1
Summary of photovoltaic performance (short-circuit current density J_{SC}, open-circuit voltage V_{OC}, fill factor *FF*, and power conversion efficiency η_P) of bilayer PbPc/C_{60} (20/40 nm) solar cells with different templating layers under 1 sun simulated solar illumination.[a]

Template	J_{SC} (mA/cm^2)		V_{OC} (V)	*FF* (%)	η_P (%)		
	Measured	Calculated[b]			Measured	Corrected[c]	Enhancement[d] (%)
None	6.0 ± 0.3	5.9 ± 0.3	0.50	53	1.59 ± 0.08	1.57 ± 0.08	–
Pentacene	9.6 ± 0.5	8.8 ± 0.4	0.50	51	2.45 ± 0.12	2.24 ± 0.11	43
CuPc	8.5 ± 0.4	7.8 ± 0.4	0.50	52	2.21 ± 0.11	2.03 ± 0.10	29
ZnPc	8.0 ± 0.4	7.1 ± 0.4	0.50	50	2.00 ± 0.10	1.78 ± 0.09	13

[a] The illumination intensity was adjusted based on the spectral mismatch factor of the non-templated device.
[b] Obtained by integrating the external quantum efficiency spectrum of the solar cell with the standard AM1.5G solar spectrum.
[c] Calculated from the calculated J_{SC} and the measured V_{OC} and *FF*.
[d] Based on the corrected η_P values.

ble 1). However, due to the variation in the EQE spectra among different devices (Fig. 5(b)), the spectral mismatch factor varies slightly from 0.95 for the non-templated device to 1.03–1.05 for the templated devices. As the solar simulator intensity was set to be 1 sun for the non-templated device in our experiments, this intensity is equivalent to approximately 1.1 suns for the device with the pentacene template. This agrees with the 10% higher calculated J_{SC} than the measured values for the template devices (see Table 1). In the subsequent discussions, we use the calculated J_{SC} along with the measured V_{OC} and *FF* to calculate a corrected power conversion efficiency that more accurately reflects the true efficiency of the templated device.

The higher content of the triclinic phase in the PbPc film grown on top of pentacene, which leads to a stronger absorption in the near infrared, is one of the reasons for the enhancement of the EQE (Fig. 5(b)) of the templated device. In addition, the internal quantum efficiency (IQE) of the templated device is also enhanced in the entire PbPc absorption spectral region. This could be attributed to the improved morphology as we discussed above: the increased crystallinity and possibly a higher hole mobility of the PbPc on the pentacene, contributing towards a higher charge collection efficiency. Furthermore, the high crystallinity obtained in the PbPc film deposited on the templating layer could also result in a higher exciton diffusion length, and therefore a higher exciton dissociation efficiency in the solar cell when a pentacene templating layer is present.

Among the various templating molecules (pentacene, CuPc, ZnPc) that we have investigated, pentacene was found to achieve the highest improvement in device performance. First, pentacene is known to form well ordered films as a material extensively used in organic transistors [22]. PbPc grown on pentacene has the highest content of the triclinic phase and the strongest absorption in the near infrared. Second, the absorption coefficient of pentacene ($\alpha = 7 \times 10^4$ cm^{-1} at the peak of absorption) is smaller than ZnPc or CuPc ($\alpha = 1.2$–2.0×10^5 cm^{-1}) [23]. The exciton diffusion length in organic semiconductors is on the order of a few nanometers [16]. When the templating layer is separated from the C_{60} acceptor by the 20 nm PbPc layer in between, it is unlikely for the excitons generated in the templating layer to diffuse to the donor–acceptor interface to dissociate. Therefore, as shown in Fig. 5(b), the EQE dips at $\lambda = 665$, 694, and 698 nm where the template pentacene, CuPc, and ZnPc absorb, respectively. Since 10 nm of ZnPc or CuPc absorbs more strongly than pentacene, the loss in the quantum efficiency due to this parasitic absorption of the template is higher, which is clearly displayed in the IQE ratio shown in Fig. 5(c).

The effect of PbPc thickness on the device performance was also investigated. The device performance and the associated EQE spectra are shown in Figs. 6 and 7, respectively. Again, the solar simulator intensity was only corrected according to the spectral mismatch for the non-templated device with a 20 nm thick PbPc, whereas η_P was corrected using the calculated J_{SC} (integrating the EQE spectra with the standard AM1.5G solar spectrum) along with the measured V_{OC} and *FF*. With or without a pentacene template, V_{OC} is nearly constant, except for the device with 10 nm PbPc on pentacene. In that case, the thin PbPc layer may not be sufficiently thick to cover the pentacene surface to form a continuous layer, such that V_{OC} is limited by the pentacene/C_{60} junction cell, which has a smaller V_{OC} [24]. Overall, without the pentacene template, a maximum η_P was obtained with 30 nm PbPc film, whereas a 20 nm thick PbPc leads to the optimum performance of $\eta_P = 2.24\%$ for devices with pentacene template.

The short-circuit current first increases as the thickness of the PbPc film increases to up to 30 nm. There is a fundamental tradeoff between the increase in optical absorption and decrease in the exciton diffusion efficiency due to the short exciton diffusion length [23,25]. In general, a further increase in the thickness of PbPc does not necessarily increase the short circuit current, but instead increases the series resistance of the device and reduces the fill factor, as shown for both cases. For the devices incorporating the template, the triclinic phase is homogenously distributed and the NIR photons are mostly absorbed in the bottom part of the film where the light first passes through, so the short circuit current rolls off right after the peak at 30 nm. On the other hand, without the templating layer, the excitons generated by the absorption of the triclinic phase are located in the middle and upper part of the film, and therefore shifts the peak of short circuit current towards a greater PbPc thickness.

We also notice that the fill factor of the non-templated device decreases more slowly as the PbPc thickness increases than the pentacene-templated device. The semi-quantitative analysis of the optical absorbance spectra

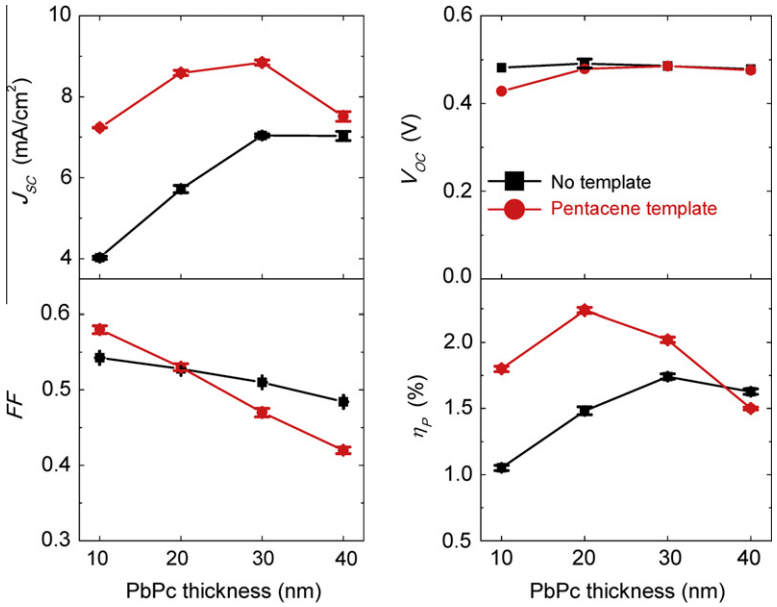

Fig. 6. Comparison of the PbPc layer thickness dependencies of the PbPc/C_{60} solar cell performance for devices with or without a pentacene templating layer.

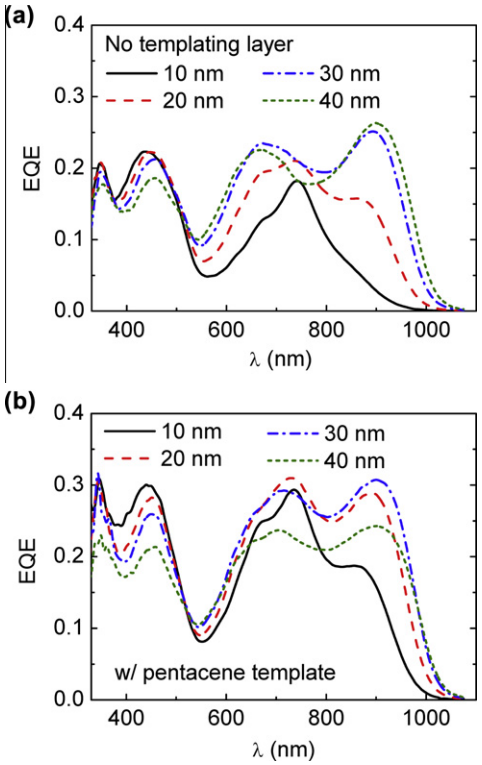

Fig. 7. The external quantum efficiency (EQE) spectra for PbPc/C_{60} solar cells with PbPc layer thickness varied from 10 to 40 nm: (a) without any templating layer and (b) with a pentacene templating layer.

mentioned earlier suggests that in the top part of a thicker film, the content of the triclinic phase for the film on the bare ITO could be higher than it is on the pentacene template. This probably contributes to a higher mobility and thus better charge collection efficiency for the non-templated device as the donor layer is more than 20 nm thick.

4. Conclusion

The morphology and crystal structure change in the PbPc film at various depths by incorporating a crystalline pentacene templating layer is investigated. The crystallinity of the PbPc film at the early stage of growth is considerably improved with templating. The content of the triclinic phase is increased as well for the typical thickness used for the bilayer solar cells. A stronger absorption in the near infrared by the triclinic phase and the enhanced internal quantum efficiency is observed for the device with a pentacene templating layer, resulting in 48% increase in the short circuit current and 42% enhancement in the power conversion efficiency. Our results demonstrate that the controlled growth of the thermally evaporated small molecular materials is a promising way to enhance the device performance.

Acknowledgements

Financial support from the National Science Foundation CAREER Program (ECCS-0644690) and Florida Energy System Consortium is gratefully acknowledged.

References

[1] J. Xue, Polym. Rev. 50 (2010) 411.
[2] A.J. Heeger, Chem. Soc. Rev. 39 (2010) 2354.
[3] J. Dai, X. Jiang, H. Wang, D. Yan, Appl. Phys. Lett. 91 (2007) 253503.
[4] R.F. Bailey-Salzman, B.P. Rand, S.R. Forrest, Appl. Phys. Lett. 91 (2007) 013508.
[5] F. Yang, R.R. Lunt, S.R. Forrest, Appl. Phys. Lett. 92 (2008) 053310.

[6] K.V. Chauhan, P. Sullivan, J.L. Yang, T.S. Jones, J. Phys. Chem. C 114 (2010) 3304.
[7] K. Vasseur, B.P. Rand, D. Cheyns, L. Froyen, P. Heremans, Chem. Mater. 23 (2011) 886.
[8] K. Ukei, Acta Crystallogr. B 38 (1982) 1288.
[9] Y. Iyechika, K. Yakushi, I. Ikemoto, H. Kuroda, Acta Crystallogr. B 38 (1982) 766.
[10] A. Miyamoto, K. Nichogi, A. Taomoto, T. Nambu, M. Murakami, Thin Solid Films 256 (1995) 64.
[11] J. Mizuguchi, G. Rihs, H.R. Karfunkel, J. Phys. Chem. 99 (1995) 16217.
[12] D. Placencia, W.N. Wang, R.C. Shallcross, K.W. Nebesny, M. Brumbach, N.R. Armstrong, Adv. Funct. Mater. 19 (2009) 1913.
[13] B.E. Lassiter, R.R. Lunt, C.K. Renshaw, S.R. Forrest, Opt. Express 18 (2010) A444.
[14] S.R. Forrest, Chem. Rev. 97 (1997) 1793.
[15] P. Peumans, V. Bulovic, S.R. Forrest, Appl. Phys. Lett. 76 (2000) 2650.
[16] P. Peumans, A. Yakimov, S.R. Forrest, J. Appl. Phys. 93 (2003) 3693.
[17] A. Ahmad, R.A. Collins, Thin Solid Films 217 (1992) 75.
[18] ASTM Standard E973, Standard Test Method for Determination of the Spectral Mismatch Parameter between a Photovoltaic Device and a Photovoltaic Reference Cell, American Society for Testing and Materials, 2002, West Conshohocken, PA, USA.
[19] F. Heringdorf, M.C. Reuter, R.M. Tromp, Nature 412 (2001) 517.
[20] S.D. Ha, A. Kahn, Phys. Rev. B 80 (2009) 195410.
[21] ASTM Standard G173-03, Standard Tables for Reference Solar Spectral Irradiances: Direct Normal and Hemispherical on 37° Tilted Surface, American Society for Testing and Materials, 2008, West Conshohocken, PA, USA.
[22] C.D. Dimitrakopoulos, P.R.L. Malenfant, Adv. Mater. 14 (2002) 99.
[23] Y. Zheng, J. Xue, Polym. Rev. 50 (2010) 420.
[24] S. Yoo, B. Domercq, B. Kippelen, Appl. Phys. Lett. 85 (2004) 5427.
[25] J. Xue, B.P. Rand, S. Uchida, S.R. Forrest, Adv. Mater. 17 (2005) 66.